

Application of the next generation of the OSCAR code system to the ETRR-2 multi-cycle depletion benchmark

M. Mashau¹, S.A. Groenewald¹, F.A. van Heerden¹

1) The South African Nuclear Energy Corporation (Necsa) SOC Ltd, Building P1900, P.O. Box 582, Pretoria, 0001 South Africa

Corresponding author: maurice.mashau@necsa.co.za

Abstract. The OSCAR code system is primarily used to perform day-to-day reactor calculations in support of the SAFARI-1 research reactor at Necsa. Recent developments in the OSCAR code focused on integrating high-fidelity and standard nodal diffusion analysis codes in a consistent way. A code independent front end system is used to create a detailed heterogeneous model of a reactor. This particular model can then be used to create input for various underlying target codes such as MCNP, Serpent and the OSCAR nodal diffusion solver (termed MGRAC), ensuring consistency between the models for target codes under consideration. The ETRR-2 benchmark, which is part of the IAEA CRP on multi-cycle depletion analysis, was modelled in aid of code validation. This benchmark is a good candidate to use for code validation because the experiments to be modelled span the first four cycles of the reactor life. All models will therefore have exactly the same initial fuel number densities, removing unnecessary uncertainty from the calculations. Prior to any burn-up, a series of control rod calibrations were performed at the plant, for which the experimental data is available in the benchmark. In this work, a detailed heterogeneous model is built in OSCAR from which a reference Serpent model is generated. In addition, cross sections and model input are also generated for use in MGRAC. Several control rod calibration experiments are simulated with Serpent to test the accuracy of the models. Depletion analysis for the four cycles is performed with Serpent and MGRAC in order to validate their burn-up capabilities. In particular, calculations are performed for three spent fuel elements. Comparisons were done between measured burn-up, Serpent and MGRAC.

1. Introduction

The OSCAR (Overall System for Calculation of Reactors) code system [1] is a nodal diffusion-based code which is primarily used to perform operational reactor calculations in support of the SAFARI-1 (South African Fundamental Atomic Research Installation number one) research reactor operated by Necsa. The code system uses a traditional deterministic approach which introduces a number of typical approximations in the process, with the level of detail for the models and calculational method decreasing at each stage. These approximations are introduced to keep the size of the reactor problem/model practically solvable.

Historically, full core fuel depletion and material activation studies have only been performed with deterministic based codes, because of their fast calculational times. However, with advances in computing power, it is now practically feasible to perform fuel depletion analysis, over multiple time steps, using Monte-Carlo based codes. Recently, a high-fidelity scheme which integrates both Monte-Carlo and deterministic modelling methods was developed as part of the next generation of the OSCAR code system (loosely termed OSCAR-5). In other words, this scheme allows reactor calculations to be performed in both high-fidelity Monte-Carlo and standard nodal diffusion analysis methods in a consistent way. This scheme can be incorporated with more traditional modelling approaches in order to improve research reactor

operational support. Research reactors in particular can benefit a lot from this high-fidelity scheme, since their cores are highly heterogeneous, making it difficult to use the traditional modelling approaches. However, deterministic based methods are still preferably used for day-to-day reactor calculations, since their computing time is appreciably lower than the more accurate Monte-Carlo based full core solvers, making them more suitable for reload analysis and for long term fuel depletion (e.g. equilibrium or fuel economy) studies.

The IAEA CRP T12029 on “Benchmarks of Computational Tools against Experimental Data on Fuel Burn-up and Material Activation for Utilization, Operation and Safety Analysis of Research Reactors”, which focuses on benchmarking computational tools against experimental data on fuel burn-up and material activation, provides a good platform for code-to-experimental comparison. This coordinated research project (CRP) is currently underway (running from 2015- 2018) and the ETRR-2 (Egyptian Testing Research Reactor number two) reactor in Egypt is one of the benchmark reactors available in the CRP. In this particular work, the scheme is used to create a detailed heterogeneous code-independent reactor model for the ETRR-2 reactor. This model is then exported to the Monte-Carlo code Serpent [2]. On the other hand, the same model is discretized and homogenized to prepare/create a cross-section library for use in MGRAC (Multi-Group Reactor Analysis Code) [1], nodal diffusion solver. In order to test the accuracy of the model, Serpent was used to perform control rod calibration experiments conducted during the commissioning phase/stage of the facility. Multi-cycle depletion analysis is performed with both Serpent and MGRAC in order to validate their burn-up capabilities.

2. Computer Codes and Methods

This section provides an overview of the codes used in this study, with specific focus on the new OSCAR-5 system. The codes used can be summarized in TABLE I.

TABLE I: Summary of codes used

| Experiment | Function | Codes used |
|------------------------|----------------------------|----------------|
| | Model Preparation | OSCAR-5 |
| Rod Calibration | Reactivity Estimation | Serpent |
| Fuel Element Depletion | Multi-cycle Fuel Depletion | Serpent, MGRAC |

2.1 Overview of OSCAR-5

The OSCAR-5 code system aims to allow for multi-code, multi-physics support for research reactor analysis, with the primary aim to facilitate the use of fit-for-purpose tools in the support of reactor operation. This implies finding a balance between the nature of a specific calculational application and the level of detail utilized in achieving the result. The OSCAR-5 system incorporates a powerful pre- and -post processing system which maintains a consistent model and manages data passing between different target codes. The main benefit and goal of the system is that, no matter which code is used, the model and input data remain consistent. *FIG.1* gives a schematic representation of the system.

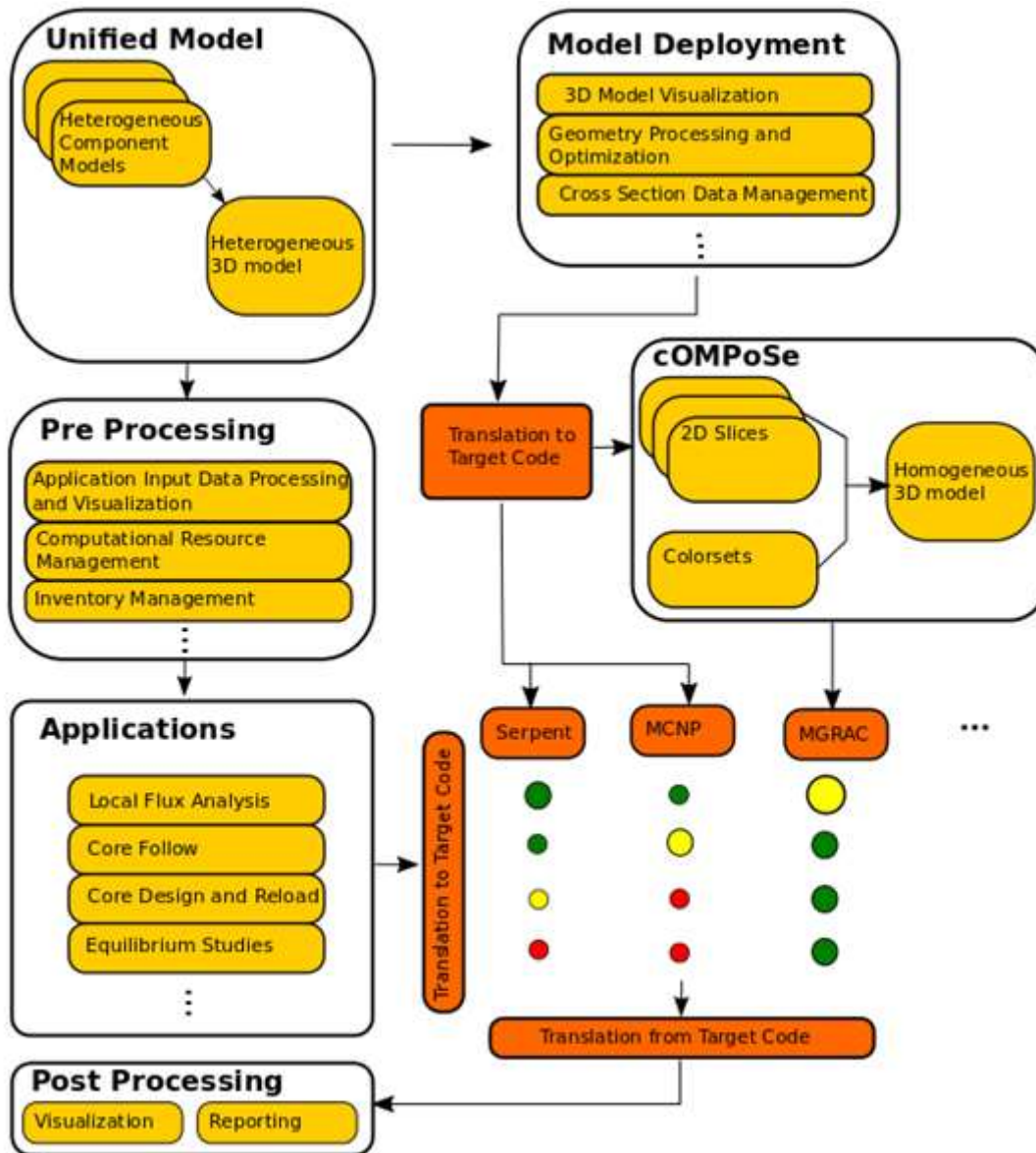


FIG.1. The OSCAR-5 code system

The entry point into the OSCAR-5 system is the building of a unified code independent model. This model can have as much detail as possible, since the geometry specifications are unconstrained. Sophisticated tools exist to assist in the model building process, such as macros for the creation of typical reactor component types, mesh optimization schemes and extensive visualization schemes.

Once a reactor model is defined, this model can be deployed to several target codes. Currently there exist translators to write the code specific model input for Serpent, MCNP [3] (Monte-Carlo N-Particle) and MGRAC. The unified heterogeneous model can be directly translated into Serpent and MCNP input but needs to go through a simplification process before it can be used in the few-group homogenized diffusion code MGRAC. This extra step in the model

preparation for MGRAC happens through the cOMPoSe (OSCAR Model Preparation System) module. More detail about cOMPoSe is given in Section 2.2.

Aside from the input preparation, OSCAR-5 is also used to deploy a model to various analysis applications. Pre-processing of data such as fuel inventory, plant data and computational resource management can be done, independent of the target code that will be used. The system also treats the input and execution of applications (such as core follow, reload safety calculations, equilibrium studies, etc.) in a code independent manner. In particular, all input data is provided through a unified system interface, with the capability to visualize and further manipulate the data.

The final deployment of an application is also handled by a set of translators for each target code. This, together with the model, provides a set of inputs for the target code. *FIG.1* lists the neutronic codes currently coupled to the system. The colour coded dots under each code illustrates the suitability of that code to the intended application. The colours ranging from green to red, indicates perfectly suitable to not recommended, respectively. The size of the dots indicates the error or level of uncertainty associated with each code for that application.

After a calculation is done, output is also translated to a unified post-processing platform for visualization and reporting.

2.2 Overview of cOMPoSe

Moving from a full detailed, heterogeneous model utilising transport theory for neutronic analysis, to coarse (or nodal) homogenized representation suitable for diffusion theory, is a fairly involved process. There are many factors to take into consideration, but the final outcome is a model with a limited number of large (assembly size) meshes which would allow for a very fast calculation of the neutron flux distribution. This model must be prepared in such a way that it captures as much of the neutronic behaviour of the heterogeneous model as possible. In the cOMPoSE system, this typically involves the following steps:

1. Since the cOMPoSe system attempts to retain as much properties as possible from the detailed model, the bulk of the homogenization process is performed on full reactor models, as opposed to single assembly models. Therefore, the first step is to select a core configuration(s) that best fit the intended purpose of the homogenized model. A coarse radial mesh is overlaid onto this chosen core configuration. This is typically done in such a way that the fuel pitch is preserved (i.e. so that fuelled assemblies fill one node).
2. Thereafter a number of radial slices are selected, axially along the length of the model, so that each slice captures important features of the model while attempting to limit the amount of axial heterogeneity within a slice. Effectively this step divides the model into a number of two dimensional layers.
3. A two dimensional transport calculation is then performed over each slice and homogenised cross sections are calculated on the nodal mesh. Generalized equivalence theory (see [4], [5]) is used to ensure that reaction rates and leakages are preserved on each node. At this point the homogenized cross sections are as accurate as possible.

4. Fuelled assemblies (or any other assemblies that either undergo state changes or get shuffled around) need additional treatment. This is because for a fast operational tool, it is not feasible to re-homogenize the entire core every time the configuration changes (such as when the core is refuelled). These assemblies are treated in a more traditional fashion, by performing assembly level lattice calculations in approximate environments, as opposed to the true full core environment. These lattice calculations also account for burnup and state changes. Since it is difficult to capture all the environments a loadable assembly would experience when generating these cross sections, this step is the major source of error in the OSCAR-5 calculational path and its effect must be carefully monitored.
5. Finally, all two dimensional layers are stacked together to form a three dimensional model. Since axial leakage is not preserved in this approach, this step introduces another potential source of error.

The OSCAR-5 system gives feedback on the errors incurred at each step during the homogenization procedure described above. By monitoring and analysing these errors during the model building phase, it is possible to quantify the accuracy of the diffusion model (MGRAC) as compared to the detailed heterogeneous model (Serpent, in this work).

3. Overview Description of the Facility and Experiments

This section gives an overview description of the ETRR-2 reactor, the experiments conducted at the reactor during the commissioning stage and details about the first four operating cycles.

3.1 Facility Description

The ETRR-2 reactor [6], [7] is a 22 MW open pool type, multi-purpose research reactor in Egypt. The facility has been used for material testing, silicon doping, medical radioisotope production, neutron activation analysis and neutron radiography [10]. It is fuelled with low-enriched (19.7 %) U_3O_8 uranium cooled and moderated with light water and reflected by beryllium blocks. The core configuration consists of a 6×5 array of 29 fuel assemblies, with 6 control blades inserted into 2 control guide boxes and a central position for cobalt irradiation. The core is surrounded by 4 chambers which can be filled with a gadolinium solution as part of the secondary reactor shutdown mechanism. The ex-core region consists of a configurable aluminium grid with beryllium blocks, hollow aluminium boxes, aluminium blocks (make up the last row of the grid positions) and a tangential beam tube surrounded by a beryllium block at the auxiliary pool side of the core. The core grid pitch is $8.1\text{cm} \times 8.1\text{cm}$ and the ex-core grid pitch is $7.87\text{cm} \times 7.87\text{cm}$.

3.2 Control Rod Calibration

During the commissioning stage of the ETRR-2 reactor, a series of control rod calibration experiments were conducted for which the results and experimental descriptions were made available in a previous IAEA CRP [7]. These experiments were conducted by moving control rods at a very low reactor power to avoid feedback effects as the reactor core will be adjusted between critical and perturbed states, with an increase/decrease in power. The control rod movements are done until the control rod which is being calibrated is fully extracted from the core. From such experiments, differential and rod worth curves can be plotted to characterize

the absorbing capability of the rod as a function of the extraction position. Since the commissioning cores and corresponding experiments consist of fresh (un-irradiated) fuel assemblies, such experiments provide a good platform to verify and validate calculational models without having to deal with extra uncertainties associated with burn-up. Core Su-29-2SO, one the commissioning cores, was chosen as a basic core configuration to test the models. Specifically, control rod 5 was calibrated using rod 3 and 6 to compensate for change in reactivity.

3.3 Fuel Burn-up Experiment

Experimental data for the first four operating cycles were made available by the benchmark supplier. The discharge burn-up of three fuel elements were measured using gamma spectroscopy. Details on the experimental set-up and measurement procedure are given in [6]. The three selected fuel elements were irradiated and removed from the core at different operational cycles. TABLE II gives an overview summary of the operational cycle relevant to this study and the properties of the three elements with measured burnup are summarized in TABLE III.

TABLE II: First four operating cycles of the ETRR-2 reactor

| Cycle Name | Full Power Days | Downtime (years) |
|------------|-----------------|------------------|
| Cycle 1 | 7.30 | 2.6 |
| Cycle 2 | 16.00 | 0.9 |
| Cycle 3 | 13.75 | 2.8 |
| Cycle 4 | 13.64 | |

TABLE III: The measured fuel elements

| Name | Initial ²³⁵ U Mass (g) | Number of Cycles in Core |
|-------|-----------------------------------|--------------------------|
| FE022 | 148.22 | 1 |
| FE014 | 148.22 | 2 |
| FE020 | 209.02 | 4 |

It was not clearly described by the benchmark supplier how the measured burn-up was calculated and therefore the following assumptions were made. An average measured burn-up is assumed for the whole assembly, and the formula for burn-up percentage was adopted from [9] and is defined as follows:

$$\text{Burnup \%} = \frac{\text{Total number of fissioned atoms}}{\text{Initial fissile atoms}} \times 100.0$$

Total number of fissioned atoms estimated using,

$$\text{Total number of fissioned atoms} \approx \sum_{c=1}^T \frac{N_{c,1} - N_{c,0}}{\gamma}$$

where T is the total number of cycles of the target assembly in the core, $N_{c,0}$, $N_{c,1}$ the number of ^{137}Cs atoms at the beginning and end of cycle c respectively, and γ is the % yield of ^{137}Cs per fission.

4. Model Description

A detailed model was prepared based on the ETRR-2 facility specification documents in [6] and [7], which includes material specifications and a geometric description of the reactor assemblies. Assembly models were created for each component in the reactor and then combined to create a complete set of different core configurations.

During the development of the reactor model, certain assumptions and simplifications had to be introduced in the process. For instance, in the case of the cobalt irradiation device, no description was provided for the spacer element, cobalt pellets loading, on material specifications for the top and bottom structure. Cobalt has a significant impact on the reactivity and therefore additional information was taken from [11]. No plant data with regard to control rod positions was provided in the benchmark and therefore critical bank searches were performed, while keeping the most two reactive rods fully extracted. The reactor power delivered was assumed to be constant throughout the operational cycles.

Three full-core models were developed for the ETRR-2 reactor. The first is the commissioning core Su-29-2SO, which was used to perform control rod calibration experiments with. The second is the first of the four operational cycles and, the last model is the second operational cycle. The ex-core structure differs for each of these cores and therefore they had to be modelled separately. No ex-core changes were made past the second operational cycle. These models were exported directly to Serpent. For the MGRAC model, additional work was required to prepare homogenized three dimensional models from the detailed heterogeneous code-independent base models as described in Section 2.1. Here only the cycle 1 model is discussed, but the procedure and results for the other configurations are similar.

The full core three dimensional model was divided into six two dimensional cuts: Two central cuts covering the active region, dividing it axially in line with the top of the ex-core tangential beam, two top reflector cuts above the core, and two bottom reflector cuts below the core. The nodal radial meshes were chosen in such a way that the main core pitch is preserved, which implies that ex-core assemblies do not necessarily fall in a single mesh. The fuel active region was axially divided into 10 exposure meshes. *FIG.2* shows the full nodal meshes and how they intersect with the base model.

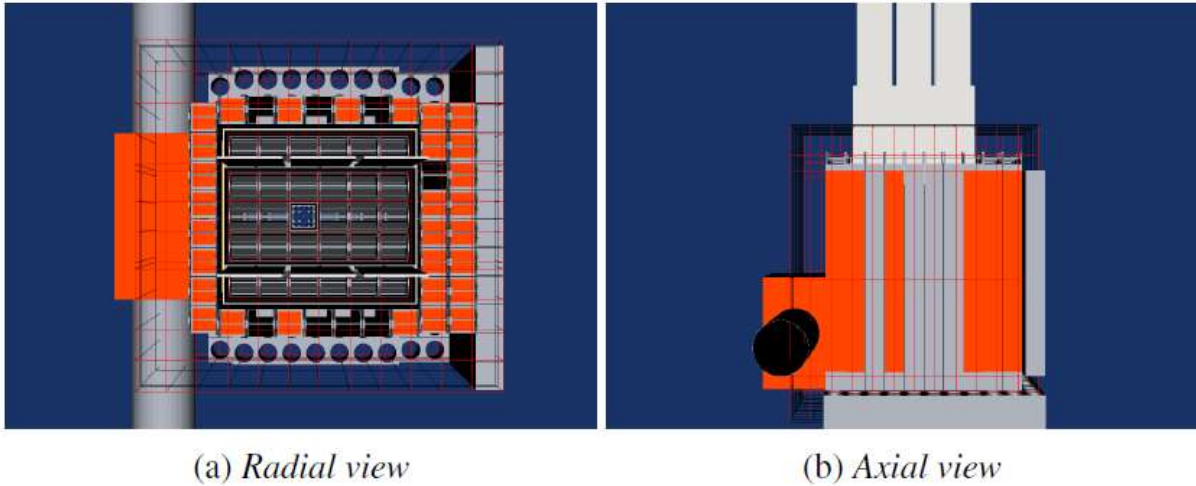


FIG.2. Overlay nodal mesh

For each two dimensional cut, Serpent was used to calculate nodal parameters on each node in the mesh for non-fuel assemblies. Control banks were extracted for central and bottom reflector cuts, while the banks were inserted for the top reflector cuts. Since fuel assembly cross sections vary with burn-up, and the assemblies are often shuffled to different positions in the core, the fuel nodes generated from the model in FIG.2 cannot be directly used. Fuel cross sections were generated in a lattice code HEADE, assuming an infinite approximate environment (fuel surrounded by other fuel assemblies). This approximation breaks full equivalence and introduces some errors into the model. The errors in the two dimensional phase of the model preparation step are summarized in TABLE IV.

TABLE IV: Two dimensional errors induced during development of the model

| Active Cut above Tangential Beam (All Rods Out) | | |
|--|--------------------------------|----------------------------|
| Reference Serpent $k_{\text{eff}} = 1.12754$ | | |
| | Reactivity Offset (pcm) | Maximum Power Error |
| Full Equivalence | -37 | 1.29 % |
| Lattice Fuel | -308 | 3.98 % |

| Active Cut (All Rods In) | | |
|---|--------------------------------|----------------------------|
| Reference Serpent $k_{\text{eff}} = 0.9650$ | | |
| | Reactivity Offset (pcm) | Maximum Power Error |
| Full Equivalence | -363 | 1.12 % |
| Lattice Fuel | -481 | 3.19 % |

For the all rods in case, the flux profile and node leakages from the core are suppressed, which makes it difficult for the diffusion based model to capture the effects. It should be noted that these two effects cause an increase of total reactivity error for the all rods in case. However, this error does not have a significant impact since all the nodal cross sections, except those for the control rods, are generated from all the rods out case. From the results, it can clearly be seen that the infinite approximation for fuel assemblies introduces notable errors into the model, and some improvements can be considered in future work in order to

reduce the errors. The full core three dimensional model was created by stacking the two dimensional mixtures on top of another. To quantify the final model error, reactivity and assembly level power distributions were compared with reference Serpent results, with rods at three positions: all rods out, all rods in and rods at 50 % extraction. See TABLE V.

TABLE V: Final three dimensional error estimation of MGRAC model

| | Reference k_{eff} | MGRAC Offset (pcm) | Max. Power Error |
|-------------------------|----------------------------|-----------------------|---------------------|
| All Rods Out | 1.07865 | -700 | 4.20 % |
| All Rods 50 % Extracted | 1.00662 | 57 | 4.00 % |
| All Rods In | 0.91106 | -647 | 3.85 % |

There is an increase in the total reactivity error for all the rods in and out cases, with an average assembly power error of about 4 %. Due to the fact that axial leakages are not preserved in the three dimensional model, this effect could have also contributed towards the error margins we see in TABLE V. Since the errors are now quantifiable, they can be refined such that one may end up with a nodal diffusion model with acceptable error margins. The first areas to refine the model are: fuel cross section generation (via more representative colorsets) and then the definition of the axial layers, so as to further reduce heterogeneities in the axial detail per layer.

5. Results and Discussion

This section contains the results for control rod calibration and fuel depletion calculations as compared to experimental measurements.

5.1 Control Rod Calibration

FIG.3 shows the control rod differential and integral curves from the selected core SU-29-2SO. It must be pointed out that for the first 13 steps, control rod 5 was calibrated using rod 3 to compensate for the change in reactivity and rod 6 was used to compensate for the remaining cases until rod 5 was completely extracted from the core. It is clearly seen from *FIG.3* that our model slightly over-estimates the measured values in most cases and under-estimates in few. Serpent results also seem to be overly sensitive to reactivity changes. This could be attributed to the fact that the fission source distribution depends on the previous case, and the reactivity estimates are therefore correlated. Thus, the error bars should be slightly larger, but this additional source of uncertainty requires further investigation.

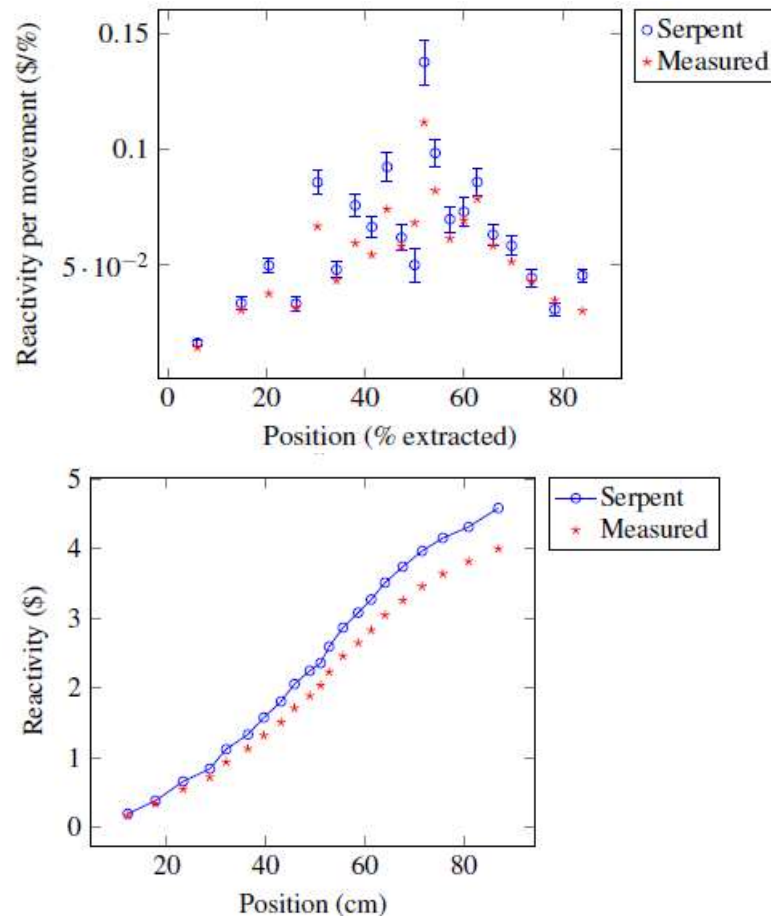


FIG.3. Control 5 calibration results (differential and integral rod worth curve)

Conceptually, the differential rod worth curve is expected to peak towards the core centre where there is a high neutron flux but in this case the flux shape is suppressed; this could possibly be due to the presence of cobalt pellets in the irradiation device. It can be clearly observed that our model deviates from the measured values.

5.2 Fuel Element Burn-up

Both Serpent and MGRAC were used to perform depletion analyses for the four operational cycles. Since no plant data with rod positions was provided, critical bank positions for rods 1, 2, 4 and 6 were searched with a target k_{eff} of 1.00150 in Serpent, and 0.99550 in MGRAC. The Serpent targeted k_{eff} was estimated based on the critical states derived from rod calibration experiments and as for the MGRAC model, the average critical k_{eff} value searched for was deduced from the cOMPOSE predictive calculations. FIG.4 shows a comparison between Serpent and MGRAC estimated critical bank positions. Rods 3 and 5, which were assumed to be the heaviest rods, were fully extracted for the entire simulation.

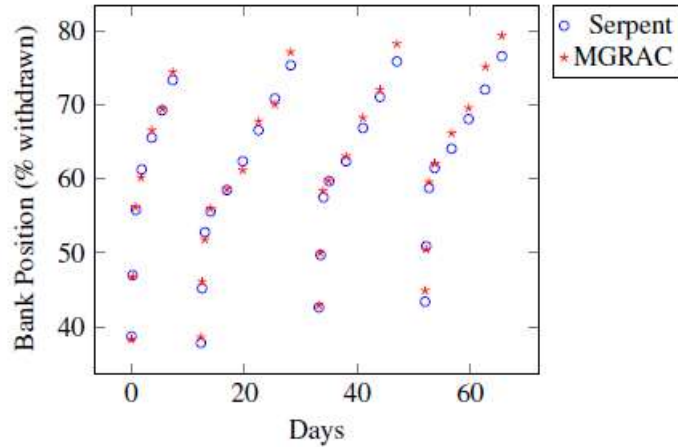


FIG.4. Critical bank positions during irradiation period

The additional existing offset between the models was estimated from the results in TABLE V and incorporated in the MGRAC model for depletion calculations. Even though the models consistently agree with each other, there is a slight offset of about ~ 2.5 % in the critical bank position towards the end of the cycles (nodal modelling errors tend to increase with burn-up since they burn differently).

TABLE VI: Burn-up of the three spent fuel elements

| Name | Measured Burn-up % | Exposure (MWd/KgU) | | Burn-up (%) | |
|-------|--------------------|--------------------|-------|-------------|-------|
| | | Serpent | MGRAC | Serpent | MGRAC |
| FE022 | 3.26 | 7.23 | 7.44 | 3.71 | 3.82 |
| FE014 | 10.07 | 22.77 | 23.19 | 11.77 | 11.98 |
| FE020 | 20.92 | 39.16 | 39.97 | 20.11 | 20.52 |

TABLE VI gives a summary of the results for the three fuel elements with the percentage burn-up estimated using the equations in Section 3.3. Both models are in good agreement with the experimentally measured values, with a maximum relative error of 17 % for assembly FE014 and dropping to below 4 % for assembly FE020. Since ^{137}Cs is not available in the WIMS-E cross section libraries used in the HEADE lattice code, the equations described in Section 3.3 cannot be used directly; therefore MGRAC burn-up percentage values were estimated by calibrating burn-up percentage to exposure in Serpent. It is not clearly described how the measured burn-up percentage was deduced from the gamma scan results. Even though the gamma scanning detector was used to measure the axial burn-up shapes, no experimental data was given, but code-to-code comparisons of estimated axial exposure is shown in FIG.5. The axial burn-up shapes are typically what one would have expected since the flux profile tends to peak towards the centre of the core.

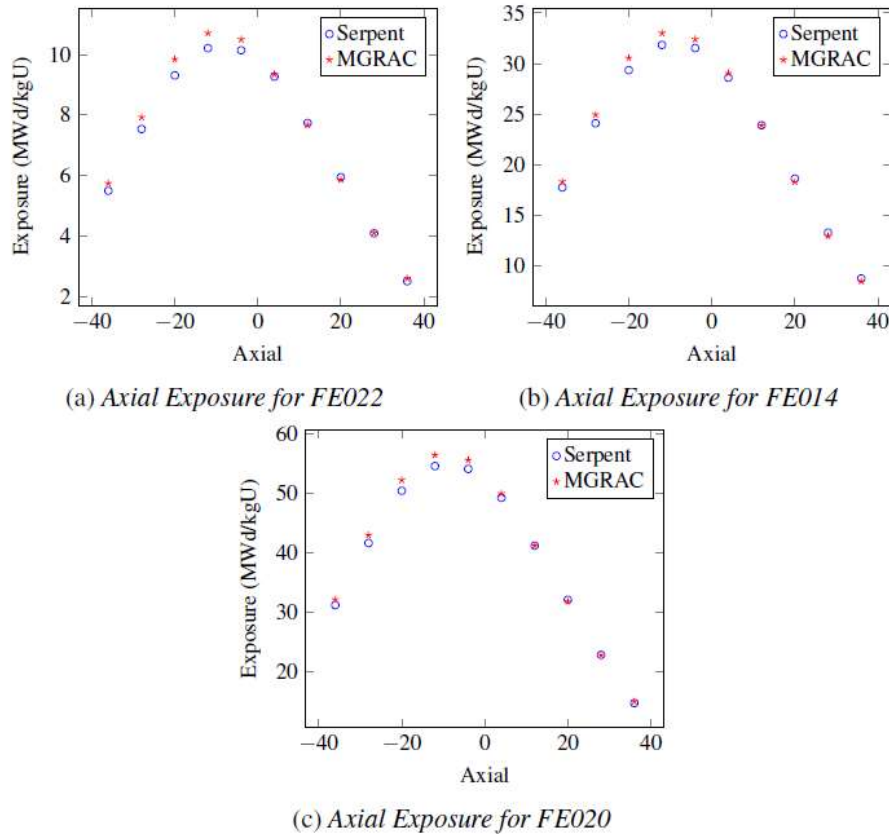


FIG.5. Code-to-code comparison of axial burn-up profiles

6. Concluding Remarks and Recommendations

This work forms part of our submission to a current IAEA CRP which focuses on benchmarking computational tools against experimental data on fuel burn-up and material activation for research reactors. Most importantly, this CRP was considered to be a good platform to test the applicability of the OSCAR-5 code system in modelling research reactors. A detailed heterogeneous code independent model was created for the ETRR-2 research reactor in Egypt (which is part of the CRP). The model was then deployed to the Monte-Carlo code Serpent and the nodal diffusion solver, MGRAC, for full core neutronic analysis. It is worth mentioning that the OSCAR-5 system significantly improved the modelling approach in the sense that errors introduced in the nodal diffusion based models are now traceable and they can be refined. Analysis was done on control rod calibration experiments that were conducted during commissioning of the reactor, as well as depletion of the first four operational cycles. The overall performance of the models was reasonably well, showing good agreement with experimental reactivity and burn-up measurements. Future work will include refining our models, especially for the fuel cross section generation as well as modelling additional control rod calibration experiments.

7. References

- [1] Stander, G., Prinsloo, R.H., Müller, E.Z., Tomašević, D.I., “OSCAR-4 Code System Application to the SAFARI-1 Reactor” International Conference on Reactor Physics,

- Nuclear Power: A Sustainable Resource, PHYSOR2008, Interlaken, Switzerland, September 14–19, 2008.
- [2] Fridman, E., Leppänen, J., “On the Use of the Serpent Monte Carlo Code for Few-Group Cross Section Generation”, *Annals of Nucl. Energy*, **38**, 1399 (2011).
 - [3] X-5 Monte Carlo Team MCNP - A General N-Particle Transport Code, Version 5 Volume I: Overview and Theory, LA-UR-03-1987 (2003, updated 2005), Los Alamos National Laboratory.
 - [4] Smith, K.S., “Assembly homogenization techniques for light water reactor analysis”, *Progress in Nuclear Energy*, 17(3):303-335 (1986).
 - [5] Sanchez, R., “Assembly homogenization techniques for core calculations”, *Progress in Nuclear Energy*, 51:14-31, (2009).
 - [6] Abdelrazek, I., Villarino, E., “ETRR-2 Nuclear Reactor: Facility Specification”, Technical report, Egyptian Atomic Energy Authority, 2014.
 - [7] IAEA Research Reactor Innovative Methods Group, “RR Benchmarking Database: Facility Specification and Experimental Data”, IAEA Technical Report Series 480, IAEA, Vienna, 2014.
 - [8] Abdelrazek, I., et.al., “ETRR-2 Fuel Burnup Evaluation”. Technical report, Atomic Energy Authority, ETRR-2, Egypt, 2014.
 - [9] Devida, C., et.al., “Quantitative Burnup Determination: A Comparison of Different Experimental Methods”, "HOTLAB" Plenary Meeting, September 6th - 8th , Halden, Norway, 2004.
 - [10] Bissani, M., Joint Assessment of ETRR-2 Research Reactor Operations Program, Capabilities, and Facilities, Technical Report UCRL-TR-221284, LLNL, 2006.
 - [11] Abou-Zaid, A.A., “Analysis of thermal neutron flux measurement in the cobalt irradiation device at ETRR-2. NUKLEONIKA, 48(4) 211-214, 2003.

